# Stability and thermophysical studies on deep eutectic solvent based carbon nanotube nanofluid

# STABILITY AND THERMOPHYSICAL STUDIES ON DEEP EUTECTIC SOLVENT BASED CARBON NANOTUBE NANOFLUID

**Yan Yao Chen[1], Rashmi Walvekar[1*], Mohammad Khalid [2], Kaveh Shahbaz [3], TCSM Gupta[4]**

[1]Energy Research Group, School of Engineering, Taylor's University, Malaysia
[2]Department of Chemical Engineering, University of Nottingham Malaysia Campus, Malaysia
[3]Department of Chemicals and Materials Engineering, University of Auckland, New Zealand
[4] Apar Industries Limited, Apar House, Corporate Park, Chembur, Mumbai 400071, India
Email: [*]rashmi.walvekar@gmail.com

**Abstract**

Commercial coolants such as water, ethylene glycol and triethylene glycol possess very low thermal conductivity,high vapor pressure, corrosion issues and low thermal stability thus limiting the thermal enhancement of the nanofluids. Thus, new type of base fluid known as deep eutectic solvents (DES) are proposed in this work as a potential substitute for the conventional base fluid due to their unique solvent properties such as low vapor pressure, high thermal stability, biodegradability and non-flammability. In this work, 33 different DESs derived from phosphonium halide salt and ammonium halide salts were synthesised. CNTs with different concentrations (0.01wt%-0.08wt%) were dispersed into DESs with the help of sonication. stability of the nanofluids were determined using both qualitative (visual observation) and quantitative (UV Spectroscopy) approach In addition, thermo-physical properties such as thermal conductivity, specific heat, viscosity and density were investigated. The stability results indicated that phosphonium based DESs have higher stability (up to 4 days) as compared to ammonium-based DESs (up to 3 days). Thermal enhancement of 30% was observed for ammonium based DES-CNT nanofluid whereas negative thermal enhancement was observed in phosphonium based DES-CNT nanofluid.

**Keywords:** Deep eutectic solvents; carbon nanotube; stability; thermal conductivity; specific heat.

## 1. INTRODUCTION

Fluids suspensed with solid nanoparticles are regarded as nanofluids and are known to improve the thermal performance of the fluid [1–3]. Some of the common nanoparticles used are copper, nickel, silver, oxides (e.g. aluminium oxides and copper oxides) and compounds such as carbon nanotube (CNT) and graphene [4-5]. CNT shows remarkably high thermal conductivity (6000 W/mK) [6] as compared to copper (401 W/m.K) and silver (429 W/mK) [7] and other metal or metal oxide nanomaterials which drastically enhances the thermal conductivity of the nanofluid [6], [8]–[11]. Due to its high thermal properties CNTs have potential applications in fields such as refrigeration, automotive and aerospace. Murshed and Nieto De Castro [6] reported that the thermal conductivity of CNT-nanofluids increases with CNT concentration and temperatures thus making nanofluids attractive heat transfer fluids at elevated temperatures.

The base fluid is also an important factor in heat transfer enhancement. The commonly used base fluids are water, engine oil and EG which have very low thermal conductivity compared to solid materials. Recently ionic liquids (ILs) have replaced commonly used base fluids. IL is a salt with poorly coordinated ions resulting in a solvent with a melting point below 100 °C. Typically they are composed of organic nitrogen containing heterocyclic cations and inorganic anions [12]. Some of its characteristics which have drawn attention of researchers from various fields are high thermal stability, high ionic conductivity, low vapour pressure and wide temperature range for liquid phase [13]. However despite of various attractive features, the application of ILs has been less favourable due to high cost and difficulty to synthesise which includes expensive raw materials and long preparation and purification procedures [14]. Hence, deep eutectic solvents (DESs) were introduced as low cost alternative of ILs [15] that are formed by mixing of halide salt with hydrogen bond donor (HBD) [16]. Up to date, the conventional applications of DESs are metal oxides dissolution

[17], electro-polishing [18], catalysis [20, 21], extraction [22–24] and electrodeposition [15]. There are no literatures available that studies DESs as heat transfer fluid.

The dispersion and stability of CNTs in base fluid is a challenge as they have the tendency to agglomerate due to Van der Waals force and strong affinity between the CNT particles [5]. Agglomerations of CNTs increases the sedimentation rate and thus decreasing the thermo-physical properties such as thermal conductivity and viscosity [24]. Various methods for nanoparticle dispersion include surface modification, surface coating and sonication. In surface modification or functionalisation, nanoparticles are oxidized using acid to attach hydroxyl (OH), carboxylic (COOH) or amine ($NH_2$) functional group to the surface through covalent bonding [5] thus increasing the interaction between nanoparticles and the based fluid. However, due to high temperature and acidic conditions during functionalisation of nanoparticles, its structures is often damaged [25]. Powerful sonication can damage and shorten the nanoparticles which in turn will decrease their mechanical properties [26]. Furthermore, surfactants disperse nanoparticles by forming a protective layer around nanoparticles and act as a barrier between them preventing agglomeration. However, the surfactant decomposes at high temperature which makes it unfit for high temperature applications. On the other hand ILs with special ionic structures has the ability to stabilise various nanoparticles without the addition of surfactant [28, 29]. ILs and DESs have been used as electrolyte, solvents for nanomaterials synthesis, exfoliation, and dispersants [29]. In recent studies, DESs were also utilised to synthesise CNT which shows improved electrocatalytic performance [30]. In addition, ammonium based DES was used to synthesise electrochemical dopamine sensor and is shown to improve the sensitivity, reproducibility and stability [31].

However, there are no studies conducted to demonstrate the potential application of DESs as heat transfer fluids. Thus, this study on DESs based CNT nanofluid reports the fundamental

thermo-physical properties is also the novelty of this paper. Hence, the objective of this study is to investigate the stability of the DESs dispersed with CNT. In addition, the thermophysical properties of the resulting nanofluids were measured to explore the potential of DESs as a replacement for conventional heat transfer fluids. This would open up more research opportunity to extend the application of DESs as a heat transfer fluid.

## 2. EXPERIMENTAL DETAILS

### 2.1. Materials

Methyl-triphenylphosphonium-bromide (MTPB) and choline chloride (ChCl) were used as the halide salts while ethylene glycol (EG) and triethylene glycol (TEG) were used as the HBDs. These chemicals were purchased from Merck, Malaysia with purity more than 99% and can be used directly for the synthesis of DESs without any further processing. In the synthesis of nanofluid, the multiwalled CNT is purchased from Chinese Academy of Science, China with more than 95% purity [5]. The nominal outer diameter of the MWCNTs is 20 nm and the length of 30 μm.

### 2.2. Preparation of DESs and CNT Nanofluid

Correct ratio of halide salt and HBD is required to form a DES. The mass of the halide salt and HBD is measured using electronic weigh balance with a precision of 1mg. The mass of both the salt and HBD varied to prepare DESs of different molar ratio given in **Table 1**. Universal laboratory bottle were used to contain the mixture of halide salt and HBD. It is important to seal off the bottle with parafilm to ensure humidity-safe environment throughout the synthesis process. This is to prevent any contamination from atmospheric moisture which may interfere with the hydrogen bonding process of the DES synthesis. The mixture is then

heated on hot plate stirrer at 80°C and 600 RPM continuously for three hours until a homogeneous colourless liquid appeared [32]. The water content in the DES was then determined using the Karl Fischer titration method (Mettler Toledo V20 Volumetric KF Titrator) via one component technique with CombiTitrant5 as the titrating agent and CombiMethanol as the working medium. As water could be intruding through the tubes and joints; hence, for precise water content measurement, the measurement started when the drift is lower than 30 µg/min. Approximately 1mL of DES sample was injected into the reaction cell and the measurements were replicated three times for each sample. The mean values of the moisture content prepared DESs in this paper are not more than 2wt%. Given that the DESs were synthesised under the atmospheric condition, and moisture from the atmosphere cannot be totally prevented and thus small amount of moisture was absorbed by the hygroscopic nature of the halide salt. However, the water content of the DESs synthesised should be within the acceptable range of less than 0.5 wt% [33, 34].

As received CNTs were measured using an analytical weigh balance with resolution of 0.0001g (MG164A, BEL Engineering) and dispersed in DES. For each of the DESs synthesised, three different concentration of CNT nanofluid were prepared as given in **Table 1**. The CNTs were dispersed using Soltec Ultrasonic Bath (Model 5300 EPS3) which operates at 37 kHz for four hours continuously at room temperature. The vibration from the ultrasonic water bath will enable the CNTs to obtain uniform and homogeneous colloid suspension. This would loosen the clustered CNTs and prevent the agglomeration.

**Table 1: Prepared CNT Nanofluids with their abbreviations**

| DES | Molar Ratio | CNT Concentration (wt%) | Abbreviation |
|---|---|---|---|
| MTPB:EG | 1:3 | 0.01 | DES 1A |
| | | 0.04 | DES 1B |
| | | 0.08 | DES 1C |
| | 1:4 | 0.01 | DES 2A |
| | | 0.04 | DES 2B |
| | | 0.08 | DES 2C |
| | 1:5 | 0.01 | DES 3A |
| | | 0.04 | DES 3B |
| | | 0.08 | DES 3C |
| MTPB:TEG | 1:4 | 0.01 | DES 4A |
| | | 0.04 | DES 4B |
| | | 0.08 | DES 4C |
| | 1:5 | 0.01 | DES 5A |
| | | 0.04 | DES 5B |
| | | 0.08 | DES 5C |
| ChCl:EG | 1:3 | 0.01 | DES 6A |
| | | 0.04 | DES 6B |
| | | 0.08 | DES 6C |
| | 1:4 | 0.01 | DES 7A |
| | | 0.04 | DES 7B |
| | | 0.08 | DES 7C |
| | 1:5 | 0.01 | DES 8A |
| | | 0.04 | DES 8B |
| | | 0.08 | DES 8C |
| ChCl:TEG | 1:3 | 0.01 | DES 9A |
| | | 0.04 | DES 9B |
| | | 0.08 | DES 9C |
| | 1:4 | 0.01 | DES 10A |
| | | 0.04 | DES 10B |
| | | 0.08 | DES 10C |
| | 1:5 | 0.01 | DES 11A |
| | | 0.04 | DES 11B |
| | | 0.08 | DES 11C |

### 2.3. Determination of CNT Stability

In order to determine the stability of the nanofluids, the synthesised nanofluids were left to stand alone without any agitation for 22 days. Visual observations were then conducted to detect any presence of suspending particles or sediment in the nanofluids. Nanofluids with presence of suspending particles or sediment are considered to be unstable. In addition to the visual observation, the concentration of nanofluids will be measured using the light intensity measurement by the UV-Vis Spectrophotometer (Model Genesys 10S) for a month [5]. First, the wavelength of the CNT is measured by identifying the peak in the absorbance spectrum

measurement. From Fig.1, the CNT wavelength is identified at 382 nm which is in good agreement with the literature [5, 35]. In order to determine the concentration of CNT in the sample, a calibration curve of absorbance value against concentration was plotted to correlate the absorbance value to the concentration. Concentration of the CNTs was then plotted against time for 22 days.

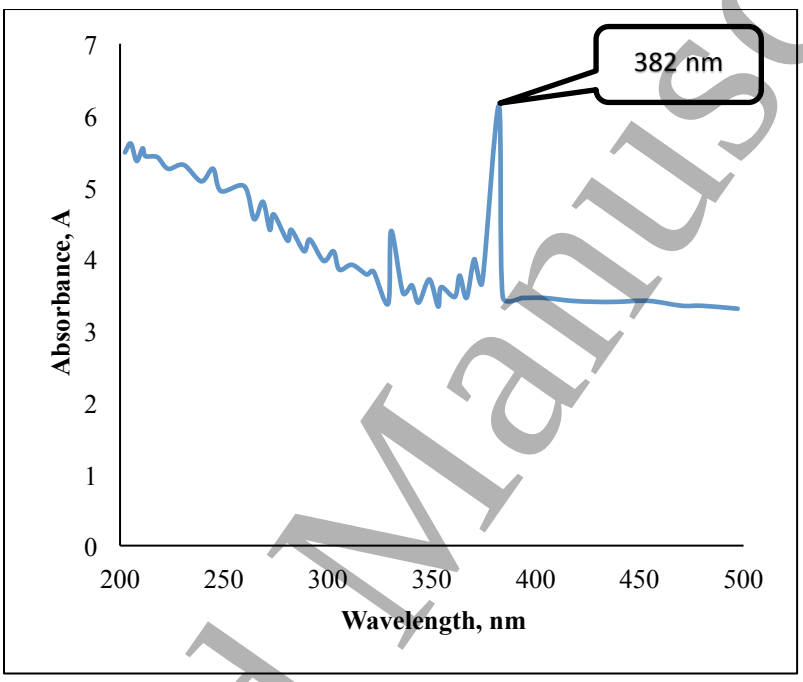


**Fig.1:** Absorbance spectrum of CNT.

### 2.4. Thermophysical Properties

Thermal conductivity, specific heat, viscosity and density of the synthesised DESs and CNT nanofluids were measured with respect to molar ratio of DESs, CNT concentration and temperature. These thermophysical properties were measured right after sonication of CNT nanofluid; therefore, the influence of clustering on the thermophysical properties is considered negligible and the CNT was uniformly dispersed.

The thermal conductivity was measured using the KD 2 Pro thermal properties analyser, (Decagon Devices, USA) with an accuracy of ± 5% and with a measuring range up to 2 W/mK. KS-1 single needle sensor was used for the measurement and the calibration was performed using the standard glycerine solution. KD2 Pro thermal properties analyser measures the thermal conductivity of the samples based on the principle of transient hot-wire method. In this method, the analyser dynamically measures the increase in temperature of a linear heat source immersed into the sample [36]. The samples were measured at different temperatures (25°C, 40°C, and 50°C) by placing the samples in a thermal jacket filled with silicon oil which is connected to a circulating thermostat bath (BL-720D) and the temperature of the bath was set to manipulate the temperature of the nanofluids. In addition, the measurement takes place inside a non-operating fume hood to isolate the sample from the influence of the ambient temperature fluctuation. The measurement of thermal conductivity was recorded at an interval of 15 minutes until three stable measurements were recorded and the average thermal conductivity was calculated.

The specific heat capacity of the pure DESs and nanofluids was determined by using the Differential Scanning Calorimeter (Model DSC 8000, Perkin Elmer). The measured heat flow is directly proportional to the specific heat capacity of the sample and can be calculated with the heat flow signal from a blank aluminium pan. Sample was measured inside an aluminium pan using analytical weigh balance with resolution of 0.0001g (Model MG164A, BEL Engineering) and recorded. The aluminium pan was then crimpled to seal the sample within the pan. The specific heat was then measured at a temperatures range of 25°C to 50°C at the heating rate of 10°C/min, which is within the recommended heating rate of the equipment [37]. In order to eliminate the noise in the heat flow signal, the sample was held at isothermal before 25°C and after 50°C for one minute.

The dynamic viscosity of the pure DESs and CNT nanofluids was measured using rheometer (Model AR2000 Rheometer, TA Instruments) with a standard double gap concentric cylinders geometry (System MK2 992291) at constant shear rate of 10 $s^{-1}$, from 20°C to 50°C temperature.

The density of the pure DESs and CNT nanofluids was measured using the Anton Paar Density Meter (Model DMA 4500M) with accuracy up to 0.00005g/$cm^3$ with standard deviation of 0.00001g/$cm^3$. The density meter was equipped with camera to ensure that there are no air bubbles in the U-tube during measurement and the nanofluid was homogeneous in the U-tube. The density of the sample is measured by the density meter via oscillating U-tube which is based on the Mass-Spring model and the mechanic oscillation of the U-tube is related to the density.

## 3. RESULTS AND DISCUSSION

### 3.1. Stability of MWCNT

Based on the visual observation, as the time passes from day 1 to day 22, the CNT nanoparticles started to sediment forming clusters of loose aggregates. This is due to the high Van der Waals force and high surface area of the CNT particles leading to agglomeration [25, 38–40]. The agglomeration then leads to increase in weight and sedimentation [3, 5]. The sediment CNT particles were observed to formed loose bundle which could easily re-disperse by merely shaking the vials. The loose bundle of CNT particles could be stipulated by the solvation of CNTs with the polar molecules of the DESs which leads to small aggregate surrounded by the DESs [41]. The small aggregate of CNTs dispersed in organic solvent forms stronger solvation which rejects any newcomer particles into the vicinity of the aggregate core [42]. Strong solvation occurs due to the reduction in conduction path and intermolecular distance and the presence of ions in the organic solvents causes higher energy

requirement for the CNT to further aggregate [41, 42]. Such phenomena does not occur in aqueous dispersions such as water due to the weak solvent molecules interaction with the inert surface of carbon [43].

The DES synthesised from EG was able to form stable CNT nanofluid for 1 day with ammonium based DESs and 3 days with phosphonium based DESs. Whereas DES synthesised from TEG is able to form stable CNT nanofluid for 3 days with ammonium based DESs and 4 days with phosphonium based DESs. This shows that usage of phosphonium based DESs are able to prolong the stability of CNT in the nanofluid. It is understood that, change in cation from phosphorus to ammonium, influence the electronic environment of the anion and thus the charge distribution. However, the influence does not seem to be very strong as the stability of the nanofluid is prolonged for phosphonium based DESs by 1 day.

In order to benchmark the effect of DESs on CNT nanofluids, CNT was also dispersed in pure EG and TEG, and were visually observed. Pure EG and pure TEG is only able to form stable CNT nanofluid for few hours. The improvement of stability is due to the increased viscosity of DES. As DES has higher viscosity compared to pure EG and TEG, this leads to higher stability of CNT nanofluids.

Figures 2 - 5 show the UV measurements indicating the sedimentation behaviour with respect to time. As seen in the figures, the concentration of CNT in nanofluids decreases with time. This indicates that the CNT starts to agglomerate over time resulting in sedimentation. The reason for the CNT being unstable is due to the Van der Waals force between the CNT particles [25, 38, 40]. The force causes the CNT particles to agglomerate together and form bigger cluster. Theses clusters are heavy and sediment due to the action of gravity.

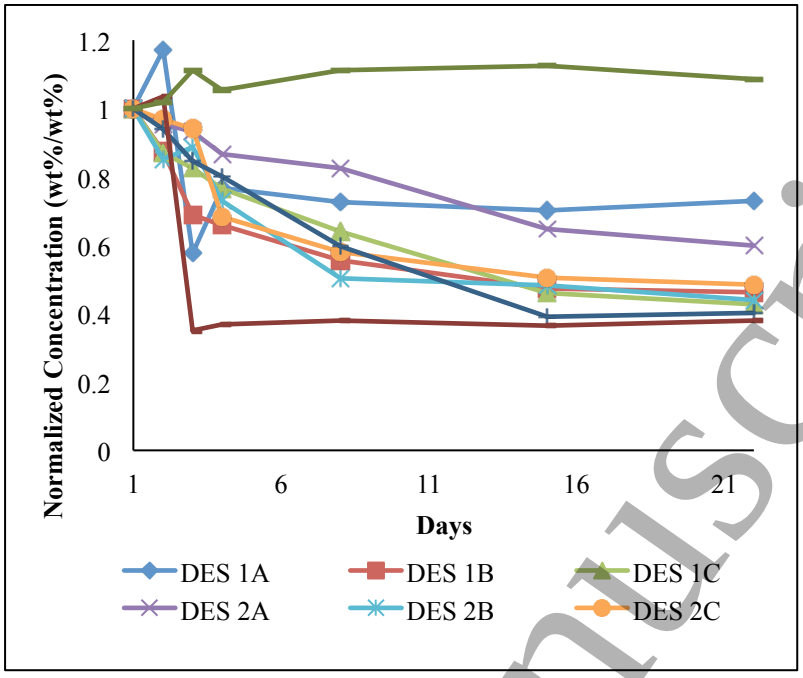


**Fig.2:** Stability of MTPB:EG based nanofluid for 22 days

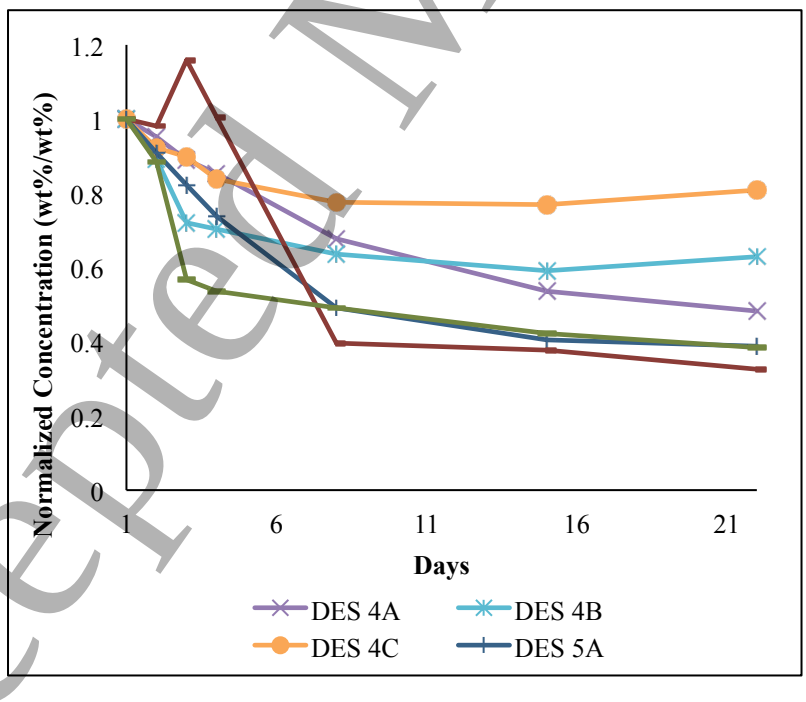


**Fig.3:** Stability of MTPB:TEG based nanofluid for 22 days

From Fig.2 it can be observed that DES 3B has a sharp decrement in concentration on the 3rd day. Similar observations were seen in Fig.2 (DES 5B) and Fig.3 (DES 7B). Another observation in Fig.4 shows that concentration of DES 9C increases in the first 5 days and decreases rapidly to a constant concentration. This is due to the fact that the UV-Vis measures the sample at a single point with the assumption that the sample is homogeneous. However, the agglomeration of CNT in the nanofluids creates a heterogeneous sample. At the instant of measurement, it is most likely that the CNT agglomerate at different localized region of the sample causing the CNT concentration at the point of measurement to decrease sharply or increase.

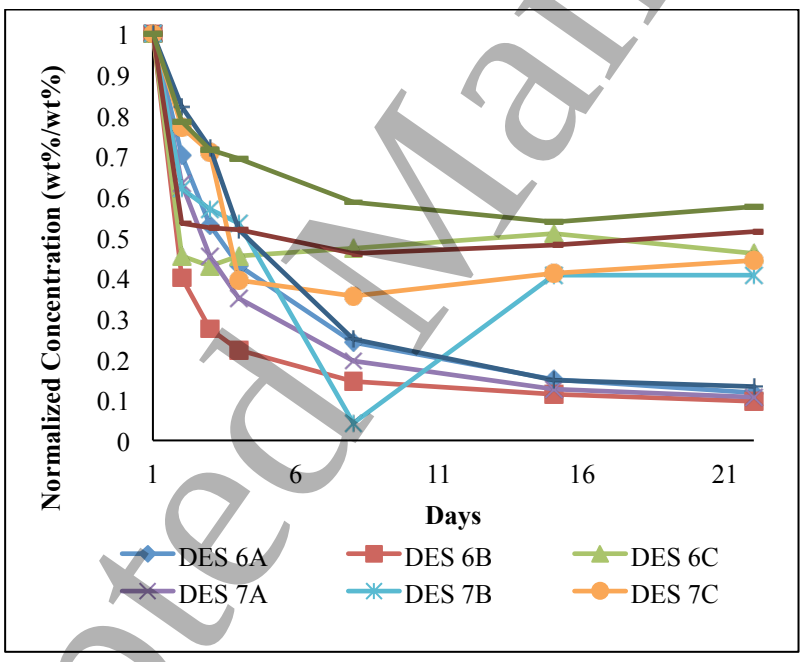


**Fig.4:** Stability of ChCl:EG based nanofluid for 22 days

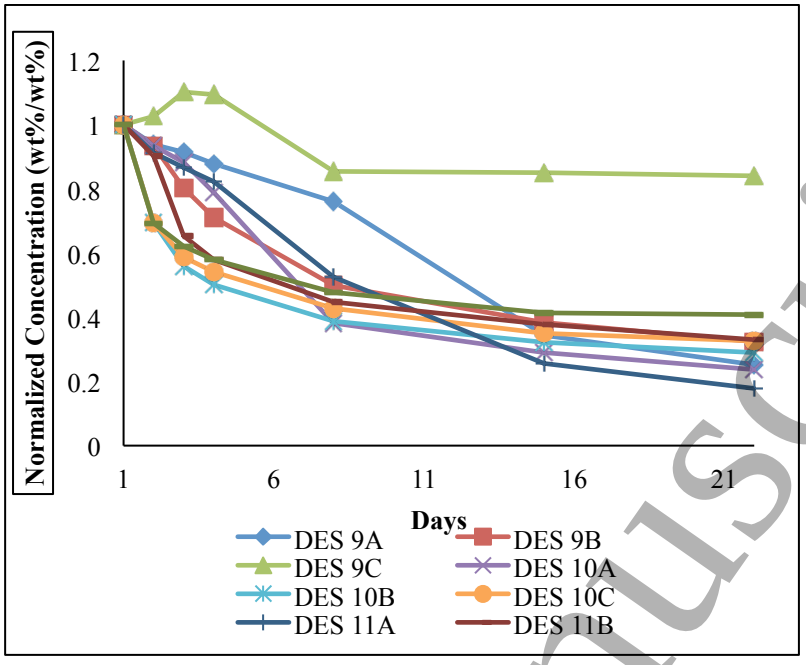


**Fig.5:** Stability of ChCl:TEG based nanofluid for 22 days

### 3.3. Thermal conductivity

Fig.6 - 16 show the thermal conductivity measurement of the samples. The measurement was restricted only up to 50°C due to the formation of large clusters that randomly moves around the sample when the temperature was increased beyond 50°C, limiting the measuring capability of the KD2 pro analyser which is only able to measure homogeneous fluid at static condition [36]. As the temperature increases, the kinetic energy and Brownian motion of the CNT particles increases as well. This causes the CNT to actively collide with each other. The Van der Waal forces then hold them together and cause agglomeration to occur [25, 38, 40]. Unwanted convection starts to occur above 50°C, which results in higher error in the thermal conductivity measurement [36, 44]. To be consistent, the thermophysical properties (specific heat, density and viscosity) were also measured at the same temperature values.

In general, the DES exhibit lower thermal conductivity compared to its respective pure organic solvents (EG and TEG) which is consistent with the is consistent with the finding of several studies reported in literature [45–47]. At temperature 25°C, phosphonium based DESs (DES 1 to DES 5) show higher negative thermal conductivity enhancement (-20.5% for DES 1, -16.9% for DES 2, -13.2% for DES 3, -12.9% for DES 4, -9% for DES 5) whereas ammonium based DESs (DES 6 to DES 11) show lower negative thermal conductivity enhancement (-7% for DES 6, -6.3% for DES 7, -5% for DES 8, -8% for DES 9, -5.4% for DES 10, -2.8% for DES 11). When the temperature is elevated to 50°C, most of the thermal conductivity enhancement of the DES improves. At temperature of 50°C, phosphonium based DESs (DES 1 to DES 5) show lower negative thermal conductivity enhancement (-15.2% for DES 1, -14.3% for DES 2, -9.9% for DES 3, -8.1% for DES 4, -7.2% for DES 5). This result is consistent with the finding on phosphonium based DES from the studies conducted by Fang et al. (2016) which shows lower thermal conductivity at temperature below 50°C. On the other hand, ammonium based DESs (DES 6 to DES 11) do not have significant changes in thermal conductivity enhancement (-7.6% for DES 6, -6.4% for DES 7, -5.4% for DES 8, -8.3% for DES 9, -5.7% for DES 10, -3.2% for DES 11). This is most likely due to the small difference in molecular weight between the ChCl (139.62 g/mol) and EG (62.07 g/mol) or TEG (150.17g/mol) as compared to MTPB (357.23 g/mol) and EG or TEG. The big difference in the molecular weight between the halide salt and HBD causes the thermal conductivity behaviour of the DESs to behave differently as the hydrogen bonding and interaction between the HBD and salt decreases [48]. As a result of that, ammonium based DESs behave similarly to its respective pure organic solvent in the increment of thermal conductivity with respect to temperature.

By dispersing CNT into the DES, the ChCl:EG DESs (DES 6 to DES 8) was able to improve its thermal conductivity enhancement from negative to positive as shown in Fig.11 to 13. The

highest thermal conductivity enhancement measured was DES 8C with 24.4% thermal conductivity enhancement at 50°C and the lowest thermal conductivity enhancement measured was DES 6A with 0.1% at 25°C. As for the ChCl:TEG DESs (DES 9 to DES 11), the thermal conductivity enhancement did not improve significantly (maximum of 2% improvement was observed). Similar observation was also observed for the phosphonium based DESs (DES 1 to DES 5). This is due to the higher viscosity of the phosphonium based DESs and ChCl:TEG DESs which restricts the Brownian motion of the CNT. With the restriction of Brownian motion, the collision between the CNT reduces and this leads to lesser solid-to-solid heat transfer and lower thermal conductivity enhancement [49, 50]. In addition, the thermal conductivity also follows the Stokes-Einstein formula which shows that the thermal conductivity is inversely proportional to the viscosity of the fluid [51]. However, in general, all nanofluids show increasing thermal conductivity with increasing CNT concentration. For instance, DES 1A which has 0.01wt% CNT shows 0.155W/mK and DES 1C which has 0.08wt% CNT shows 0.161W/mK at 25°C. These trend are consistent with the trend obtained from literatures [5, 6, 9, 46]. For constant CNT concentration, all nanofluids also show increasing thermal conductivity with increasing temperature. As shown in Fig.6, DES 1A has thermal conductivity of 0.155W/mK at 25°C and 0.162W/mK at 50°C. Similar trend was observed for all nanofluids synthesised. The non-linear increment of thermal conductivity with respect to temperature is consistent with the findings in literatures [8, 39, 52–54].

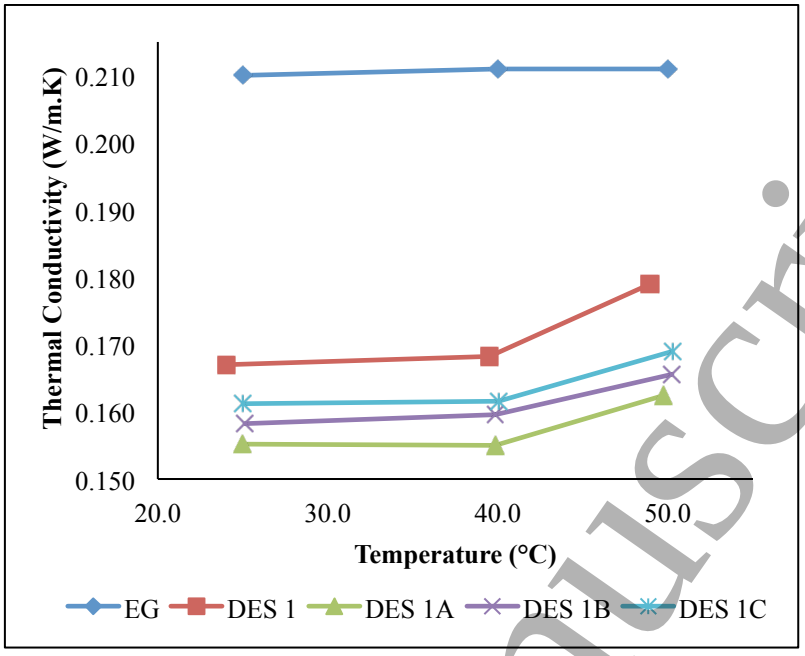


**Fig.6:** Thermal conductivity of DES 1 and its CNT nanofluid

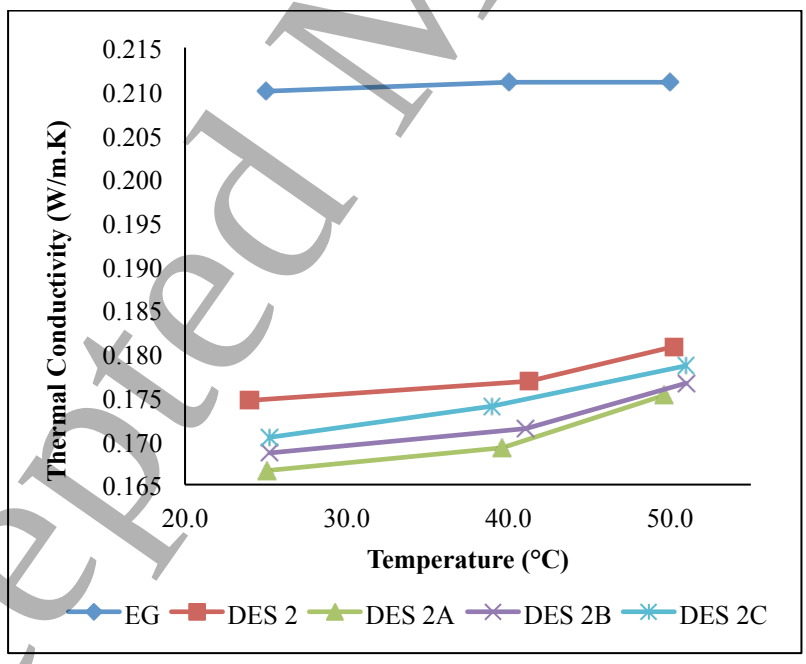


**Fig.7:** Thermal conductivity of DES 2 and its CNT nanofluid

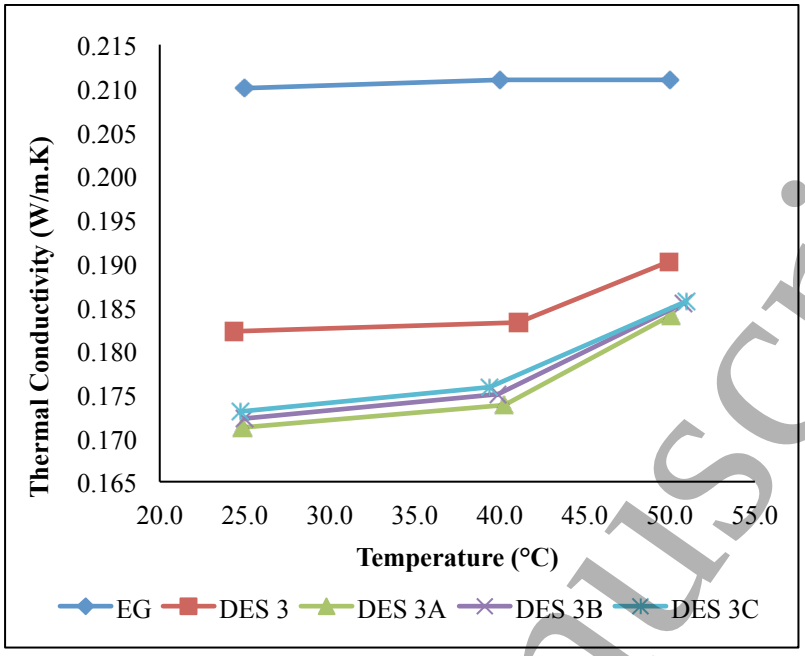


**Fig.8:** Thermal conductivity of DES 3 and its CNT nanofluid

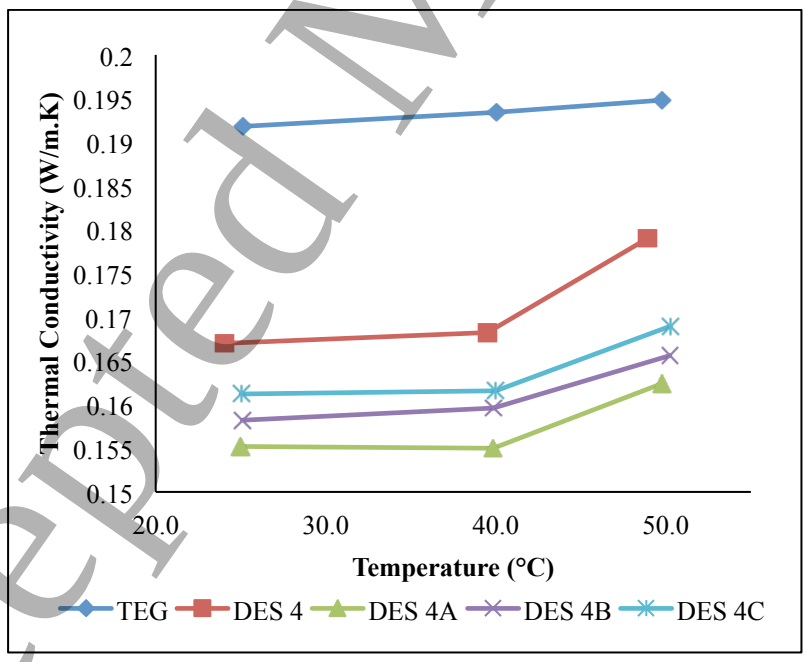


**Fig.9:** Thermal conductivity of DES 4 and its CNT nanofluid

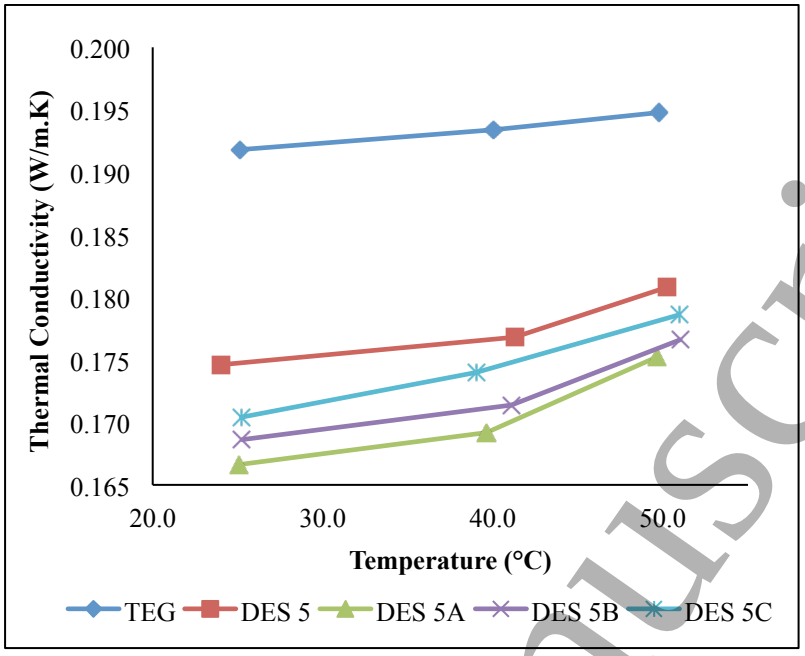


**Fig.10:** Thermal conductivity of DES 5 and its CNT nanofluid

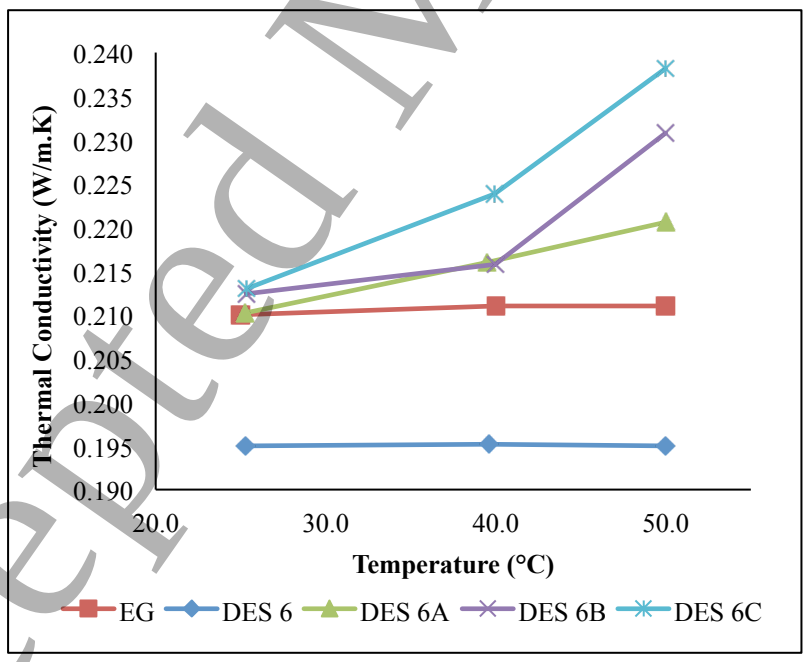


**Fig.11:** Thermal conductivity of DES 6 and its CNT nanofluid

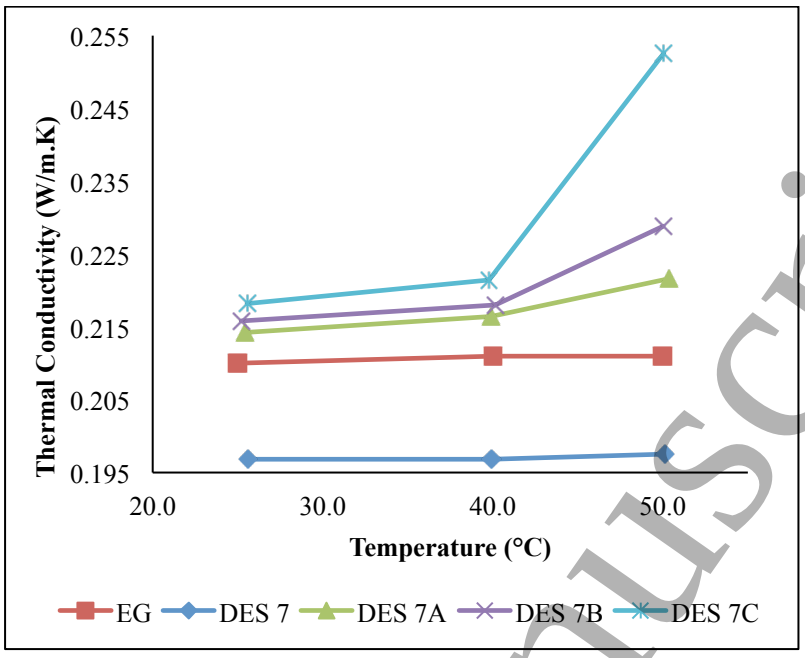


**Fig.12:** Thermal conductivity of DES 7 and its CNT nanofluid

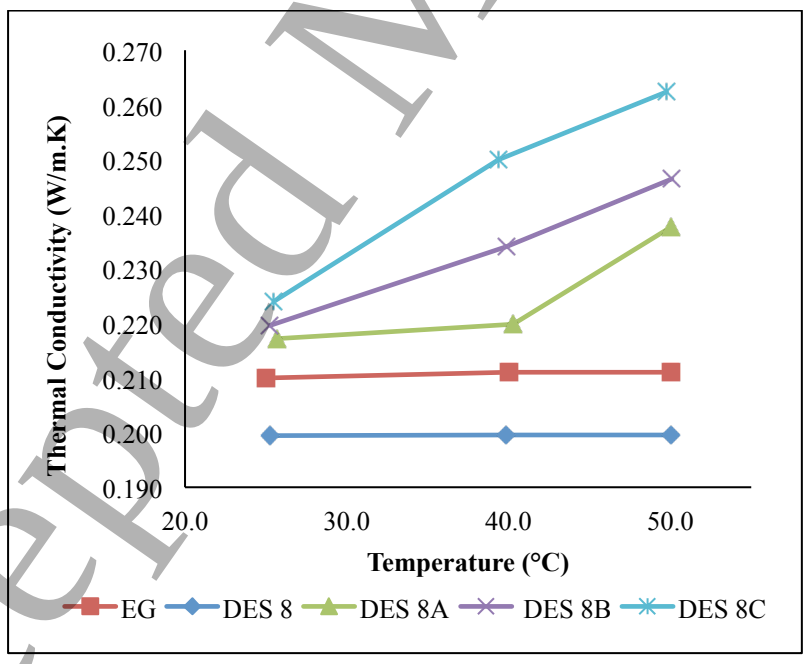


**Fig.13:** Thermal conductivity of DES 8 and its CNT nanofluid

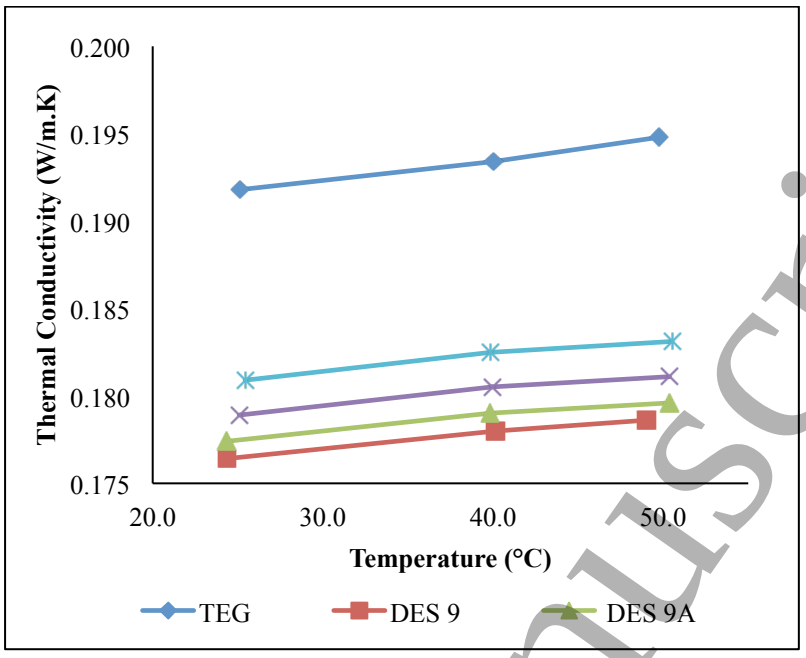


**Fig.14:** Thermal conductivity of DES 9 and its CNT nanofluid

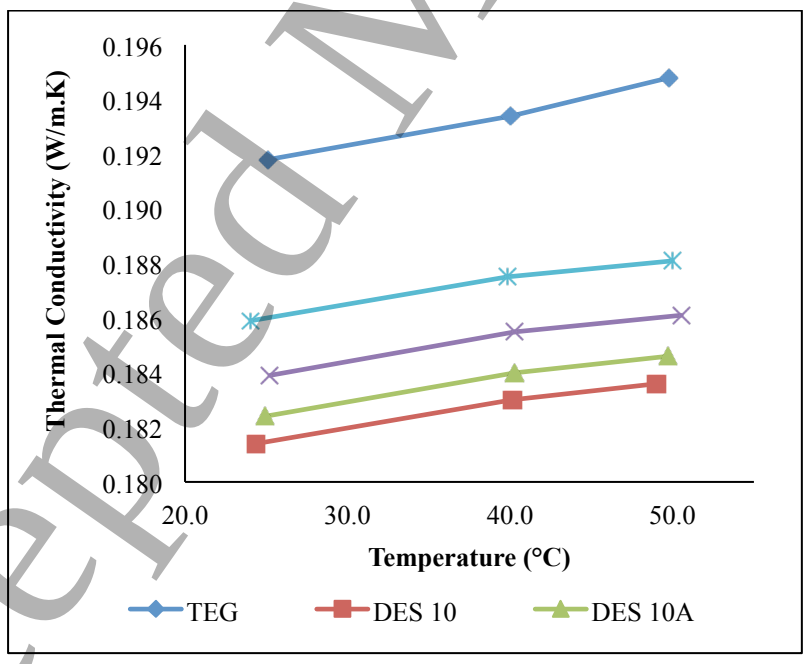


**Fig.15:** Thermal conductivity of DES 10 and its CNT nanofluid

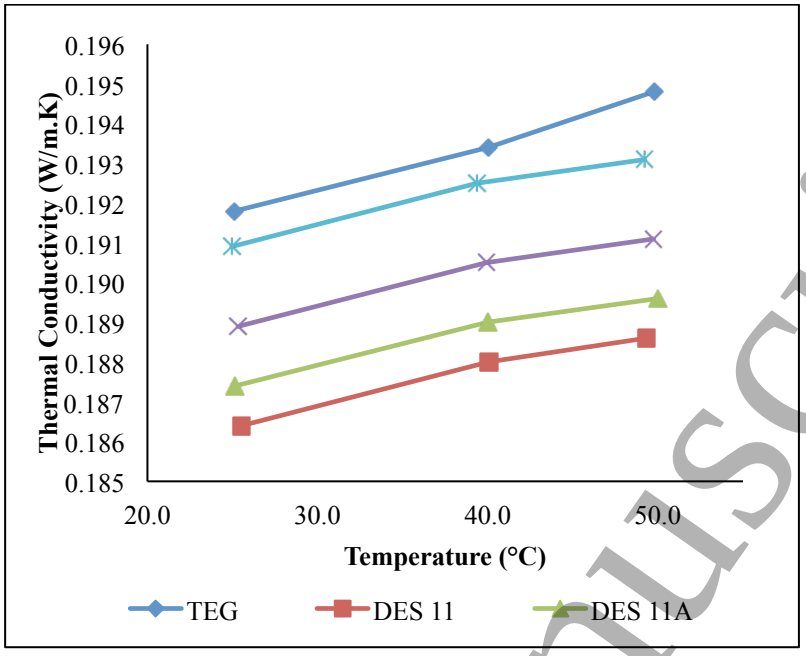


**Fig.16:** Thermal conductivity of DES 11 and its CNT nanofluid

### 3.4. Specific Heat

CNT nanoparticle concentration plays critical role in the heat capacity changes because of the changes in the phonon vibration mode at solid-liquid interface [55]. As the CNT nanoparticle concentration increases, the specific heat capacity of the nanofluid was found to decrease as shown in Fig.17 for DES 1 and its nanofluid. As most of the specific heat of the DESs and its nanofluid follows the same trend, only one figure was shown to represent the nanofluid studied in this work.

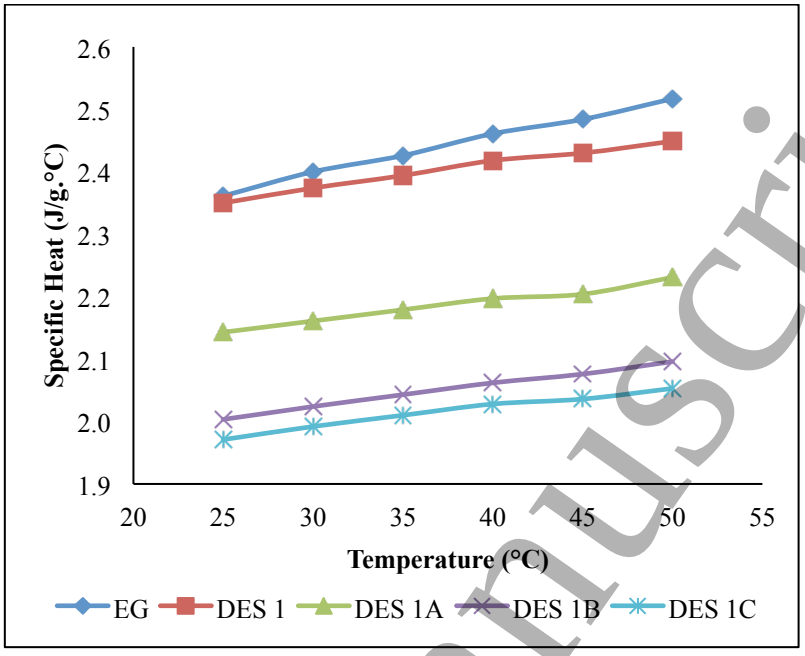


**Fig.17:** Specific heat of DES 1 and its CNT nanofluid

The decreasing specific heat capacity in DES is consistent with a study conducted on 1-hexyl-3-methylimidazolium tetrafluoroborate (HMIM]BF4) with graphene nanoparticles by Liu et al. (2014), wherein the graphene concentration was increased from 0.03 - 0.06wt% while the specific heat of the ionanofluid decreased by 3% [45]. Such a behaviour can be explained by the constrained liquid layering at the surface of nanoparticle free boundary which causes the variations in the Gibbs free energy and thus affects the specific heat capacity [56]. The decreased in specific heat can also be explained due to the additional thermal storage mechanisms from the interfacial interactions, such as the interfacial thermal resistance and capacitance, between nanoparticle and the adhering liquid molecules which arises due to the large specific surface area of the nanoparticles [56]. Therefore, as the CNT cluster size increases (due to the increase in CNT concentration), the specific surface area of

the nanoparticles would decreases sharply. This causes the nanoparticle to have surface specific energy similar to its bulk materials (which is lower than the surface specific energy of the nanoparticle), which ultimately decreases the specific heat of the resulting nanofluid [45, 55, 57]

Fig.18 and Fig.19 show the specific heat of the synthesised DES in comparison with its respective pure organic solvents (EG and TEG). Naser et al [57] studied the molar heat capacity of type III DES's and showed that the heat capacity is directly proportional to the molar ratio of the DES. For the EG based DES shown in Fig.17, only DES 1 shows lower specific heat than its pure organic solvent, which could be possibly due to lower molar mass of HBD. The specific heat of DES increased with molar mass due to increase in the number of free translational, vibrational and rotational modes in the HBD [58]. The specific heat capacity enhancement of the EG based DES, at 50°C, in ascending order are DES1 (-2.7%) > DES2 (-0.1%) > DES3 (2.6%)> DES6 (2.8%) >DES7 (6.1%) > DES8 (7.3%). Similarly, the TEG based DES also exhibit similar characteristics. The specific heat capacity enhancement of the TEG based DES, at 50°C, in ascending order are DES4 (0.9%) > DES5 (3.9%) > DES9 (4.4%)> DES 10 (5.1%) >DES 11 (6.0%), respectively.

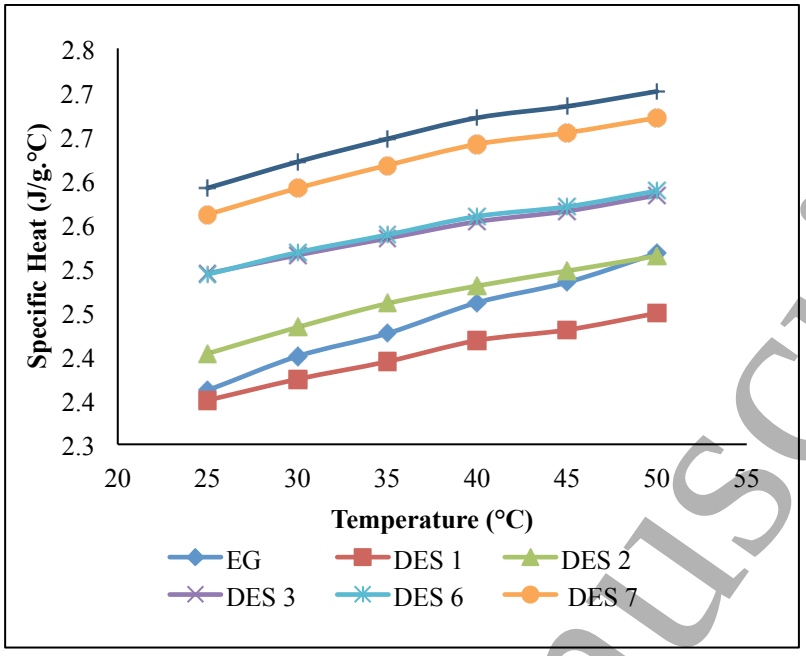


**Fig.18:** Specific heat of EG based DES

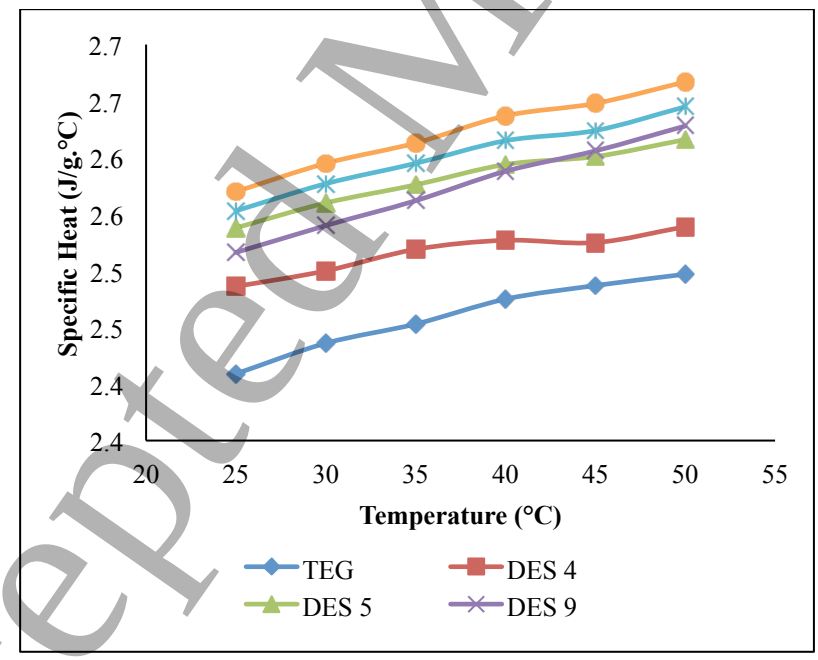


**Fig.19:** Specific heat of TEG based DES

### 3.5. Viscosity

Fig.20 shows the viscosity of the DES 1 and its nanofluid at constant shear rate ($10s^{-1}$) with respect to temperature. Only one figure was used to represent the viscosity trend of all the samples studied in this paper due to its similarity in trend. From Fig.19, the viscosity of the DESs and its nanofluid reduces with increasing temperature. This indicates that the DESs and its nanofluids follow the Arrhenius behaviour [17] and the trend is in a good agreement with the reported trend in literature [3, 48, 54].

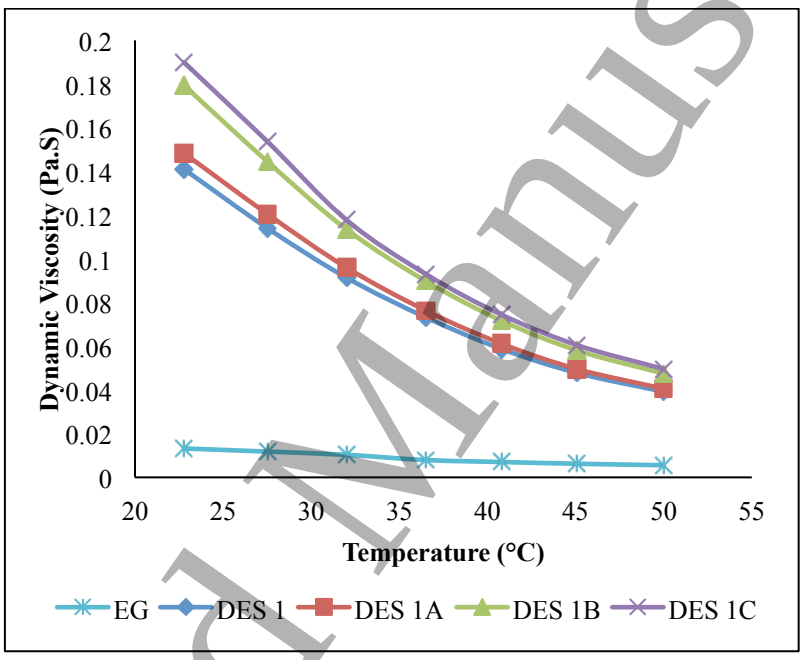


**Fig.20:** Dynamic viscosity of DES 1 and its CNT nanofluid

The decreasing viscosity trend was due to higher intermolecular forces at higher temperature and it is observed that the DESs mixture begin to converge into the viscosity of the respective pure organic solvents. It was also observed that most of the DES has viscosity higher than 25cP at room temperature which is higher than the pure organic solvents, EG and TEG. This is because the extensive and complex hydrogen bonding between the halide salt and HBD which causes the DESs to be less mobile and have higher viscosity [15, 48, 60]. The

increment in viscosity is highly due to the chemical nature of its component such as the molar ratio, type of halide salt and the HBD [17]. This explains, for every DES variation, the increased in viscosity with decreasing molar ratio (1:5 to 1:3). This is also in agreement with the results obtained in literature that shows higher viscosity for lower molar ratio [18, 48, 61]. DES synthesised from the MTPB salt has higher viscosity compared to the DES synthesised from ChCl salt. This is because the DES synthesised from MTPB salt requires more salt to achieve the desired molar ratio whereas DES synthesised from ChCl salt requires lesser salt at the similar molar ratio. This is generally generates more extensive hydrogen bonding between the halide salt and HBD which leads to higher viscosity [48].

When the CNT is dispersed into DES to form CNT/DES nanofluid, the viscosity of the resulting nanofluid increased even higher that it's respective DES. The increased viscosity of CNT/DES nanofluid is due to the higher Van der Waals interaction between the CNT nanoparticles. As shown in Fig.19, DES 1C has the highest viscosity compared to DES 1B and DES 1A. Similar trend is observed in all CNT/DES nanofluid. These effect of CNT nanoparticle concentration on the viscosity of the CNT/DES nanofluid is consistent with the finding in literatures [3, 53, 62]. For instance, a study conducted by Das et al (2003) shows that the viscosity increases with increase in nanoparticle concentration. In addition to the CNT concentration, CNT nanoparticle size can also be one of the factor that causes the viscosity to increase with increasing CNT concentration [62]. The CNT nanoparticle size increased with increasing CNT concentration due to agglomeration. The larger cluster of CNT nanoparticle causes increment in friction which resulted in higher measured viscosity.

### 3.6. Density

Fig.21 shows the measured density of the DES 1 with respect to different CNT concentration. Only one figure was used to represent the density trend of all the samples studied in this paper due to its similarity. The measured density of the CNT/DES nanofluid increases with

increasing CNT concentration. As the density of the CNT nanoparticle is higher than liquids, therefore, the density of the nanofluid would generally increases with the addition of CNT nanoparticles. The increasing trend in density is consistent with the mixing theory of ideal gas mixture and with the study done by Pakdaman et al. (2012) on CNT/water nanofluids that shows increasing density of the nanofluid with increasing CNT concentration.

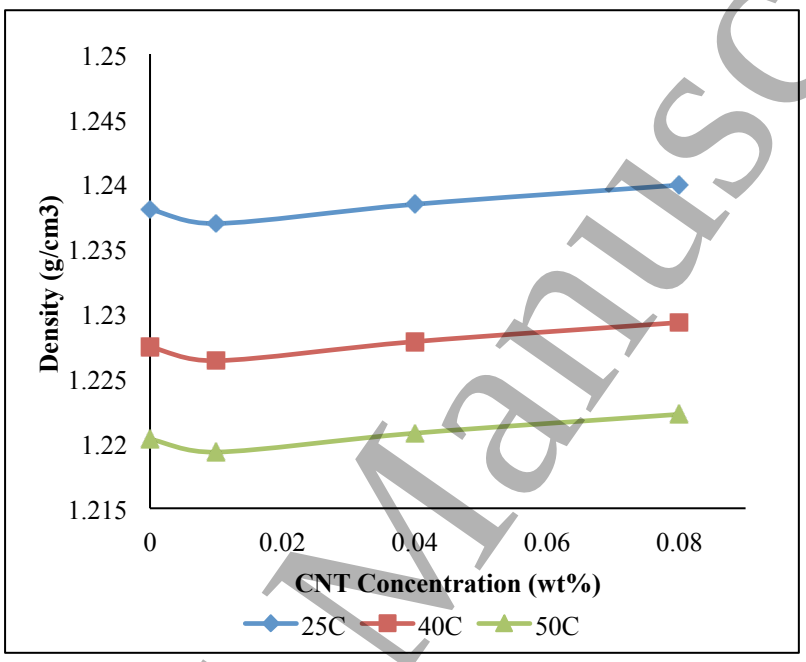


**Fig.21:** Density of DES 1 and its CNT nanofluid

It was also observed that when the CNT was dispersed into the DES, there is a slight drop in density. The slight drop in density is due to the difference in eigenfrequency between a liquid mixture and a solid-liquid mixture. The difference was due to the calibration that was done under the assumption of a single phase mixture. Regardless, the density of the CNT/DES nanofluid measured is within the experiment uncertainty (less than 0.01g/cm$^3$). In addition to the effect of CNT on the density, the molar ratio of the DES can also be related to the density of the DES. As the molar ratio of the DES decreases (from 1:5 to 1:3), the density of the DES

would increase accordingly. This is due to the higher density of the halide salt. As more halide salt is present in the DES mixture, the density of the DES would increases.

## CONCLUSION

In this study, MTPB, ChCl, EG and TEG are used to produce DES to serve as the base fluid for DES/CNT nanofluid formulation. The results show that DES/CNT nanofluid is unable to overcome the attractive forces between CNT nanoparticles, which led to sedimentation in all prepared nanofluids in a short period. However, presence of salt is in HBD able to provide higher stability compared to its respective pure organic solvents. From the visual observation and UV-vis spectrophotometer, it was also observed that the MTPB based DES is able to form stable CNT nanofluid for a longer period (up to 4 days) compared to ChCl based DES (up to 3 days). Positive thermal conductivity enhancement was only observed for the DES/CNT nanofluid derived from ChCl:EG with the highest thermal conductivity enhancement measured of 24.4% at 50°C. The specific heat of the DES/CNT nanofluid was observed to be lower than the specific heat of its pure organic solvent due to the lower heat storage mechanism of the solid nanoparticles and the halide salt used in the DES formulation. Addition of salt increased the viscosity compared to the pure organic solvents, EG and TEG due to the extensive and complex hydrogen bonding, and higher Van der Waals interaction between the CNT nanoparticles. The measured density of the CNT/DES nanofluid increases with increasing CNT concentration and the variation in density varies significantly based on the type of DES used and has insignificant relation to the CNT concentration. Therefore, as the molar ratio of the DES decreases (from 1:5 to 1:3) the density of the DES would increase accordingly.

It is conclusive that DES/CNT nanofluids derived from MTPB halide salt are able to provide higher stability to the DES/CNT nanofluid with the cost of higher viscosity and negative thermal conductivity enhancement. On the other hand, DES/CNT nanofluids derived from

ChCl halide salt offer lower stability but with less increment in viscosity and positive thermal conductivity enhancement.

**ACKNOWLEDGEMENT**

The authors would like to acknowledge the Ministry of Higher Education (MOHE) for the financial funding through Fundamental Research Grant Scheme FRGS-FRGS/2/2013/TK06/TAYLOR/03/1).

**REFERENCES**

[1] M. Assael, I. Metaxa, K. Kakosimos, and D. Constantinou, "Thermal conductivity of nanofluids – experimental and theoretical," *Int. J. Thermophys.*, vol. 27, pp. 999–1016, 2011.

[2] S. Das, S. Choi, and H. Patel, "Heat transfer in nanofluids—A review," Feb. 2007.

[3] Y. Ding, H. Alias, D. Wen, and R. Williams, "Heat transfer of aqueous suspensions of carbon nanotubes (CNT nanofluids)," *Int. J. Heat Mass Transf.*, vol. 49, pp. 240–250, 2006.

[4] I. . Mahbubul, R. Saidur, and M. . Amalina, "Influence of particle concentration and temperature on thermal conductivity and viscosity of Al2O3/R141b nanorefrigerant," *Int. Commun. Heat Mass Transf.*, no. 43, pp. 100–104, 2013.

[5] W. Rashmi *et al.*, "Stability and thermal conductivity enhancement of carbon nanotube nanofluid using gum arabic," *J. Exp. Nanosci.*, vol. 6, pp. 567–579, 2011.

[6] S. Murshed and C. Nieto de Castro, "Superior thermal features of carbon nanotubes-based nanofluids - A review," *Renew. Sustain. Energy Rev.*, vol. 37, pp. 155–167, 2014.

[7] S. Choi and J. Eastman, "Enhancing thermal conductivity of fluids with nanoparticles," in *ASME International Mechanical Engineering Congress & Exposition*, 1995.

[8] M. De Volder, S. Tawfick, R. Baughman, and A. Hart, "Carbon nanotubes: present

and future commercial applications.," *Science (80-. ).*, vol. 339, pp. 535–9, Feb. 2013.

[9] H. Xie and L. Chen, "Review on the preparation and thermal performances of carbon nanotube contained nanofluids," *J. Chem. Eng. Data*, vol. 56, pp. 1030–1041, Apr. 2011.

[10] W. Rashmi, M. Khalid, S. Ong, and A. Ismail, "Application of CNT nanofluids in a turbulent flow heat exchanger," *J. Exp. Nanosci.*, 2015.

[11] W. Rashmi, I. Faris, and M. Khalid, "Thermal conductivity of carbon nanotube nanofluid-Experimental and theoretical study," *Heat Transf. Res.*, vol. 41, pp. 145–163, 2012.

[12] A. A. Shamsuri and D. K. Abdullah, "Ionic Liquds: Preparations and Limitations," *Makara Sains*, vol. 14, no. 2, pp. 101–106, 2010.

[13] A. Matic and B. Scrosati, "Ionic liquids for energy applications," *MRS Bull.*, vol. 38, no. 7, pp. 533–537, Jul. 2013.

[14] K. Shahbaz, F. Mjalli, M. Hashim, and I. AlNashef, "Prediction of deep eutectic solvents densities at different temperatures," *Thermochim. Acta*, vol. 515, pp. 67–72, Mar. 2011.

[15] E. Smith, A. Abbott, and K. Ryder, "Deep eutectic solvents (DESs) and their applications," *Chem. Rev.*, vol. 114, pp. 11060–11082, 2014.

[16] Y. Dai, G. . Witkamp, R. Verpoorte, and Y. Choi, "Natural deep eutectic solvents as a new extraction media for phenolic metabolites in carthmux tinctorius L," *Anal. Chem.*, vol. 85, pp. 6272–6278, 2013.

[17] Q. Zhang, K. Oliveir Vigier, S. Royer, and F. Jérôme, "Deep eutectic solvents: synthesis, properties and applications," *Chem. Soc. Rev.*, vol. 41, pp. 7108–7146, 2012.

[18] A. Abbott, K. Ttaib, G. Frisch, K. Ryder, and D. Weston, "The electrodeposition of silver composites using deep eutectic solvents," *Phys. Chem. Chem. Phys.*, vol. 7, pp.

2443–2449, 2012.

[19] D. Lindberg, M. Fuente Revenga, and M. Widersten, "Deep eutectic solvents (DESs) are viable cosolvents for enzyme-catalyzed epoxide hydrolysis," *J. Biotechnol.*, vol. 3–4, pp. 169–171, 2010.

[20] H. Zhao, C. Zhang, and T. Crittle, "Choline-based deep eutectic solvents for enzymatic preparation of biodiesel from soybean oil," *J. Mol. Catal. B Enzym.*, vol. 85–86, pp. 243–247, 2013.

[21] A. Abbott, P. Cullis, M. Gibson, R. Harris, and E. Raven, "Extraction of glycerol from biodiesel into a eutectic based ionic liquid," *Green Chem.*, vol. 8, pp. 868–872, 2007.

[22] R. Leron and M. Li, "Solubility of carbon dioxide in a choline chloride–ethylene glycol based deep eutectic solvent," *Thermochim. Acta*, vol. 551, pp. 14–19, 2013.

[23] R. Leron, A. Caparanga, and M. Li, "Carbon dioxide solubility in a deep eutectic solvent based on choline chloride and urea at T = 303.15–343.15 K and moderate pressures," *J. Taiwan Inst. Chem. Eng.*, vol. 6, pp. 879–885, 2013.

[24] A. Ghadimi, R. Saidur, and H. Metselaar, "A review of nanofluid stability properties and characterization in stationary conditions," *Int. J. Heat Mass Transf.*, vol. 54, pp. 4051–4068, 2011.

[25] W. H. Chang, I. W. Cheong, S. E. Shim, and S. Choe, "The dispersion stability of multi-walled carbon nanotubes in the presence of poly(styrene/α-methyl styrene/acrylic acid) random terpolymer," *Macromol. Res.*, vol. 14, no. 5, pp. 545–551, 2006.

[26] L. F. Dumee, "Carbon-nanotube-based membranes for water desalination by membrane distillation," Victoria University, Melbourne, Australia, 2011.

[27] M. L. Polo-Luque, B. M. Simonet, and M. Valcárcel, "Functionalization and dispersion of carbon nanotubes in ionic liquids," *TrAC Trends Anal. Chem.*, vol. 47, pp.

99–110, Jun. 2013.

[28] A. Wittmar and M. Ulbricht, "Dispersions of Various Titania Nanoparticles in Two Different Ionic Liquids," *Ind. Eng. Chem. Res.*, vol. 51, no. 25, pp. 8425–8433, Jun. 2012.

[29] A. Abo-Hamad, M. Hayyan, M. AlSaadi, and M. Hashim, "Potential applications of deep eutectic solvents in nanotechnology," *Chem. Eng. J.*, vol. 273, pp. 551–567, Aug. 2015.

[30] R. Wang, Y. Fan, Z. Liang, J. Zhang, Z. Zhou, and S. Sun, "PdSn nanocatalysts supported on carbon nanotubes synthesized in deep eutectic solvents with high activity for formic acid electrooxidation," *RSC Adv.*, vol. 6, pp. 60400–60406, 2016.

[31] L. Wu *et al.*, "Dopamine sensor based on a hybrid material composed of cuprous oxide hollow microspheres and carbon black," *Microchim. Acta*, vol. 182, pp. 1361–1369, 2015.

[32] A. Abbott, D. Boothby, G. Capper, D. Davies, and R. Rasheed, "Deep eutectic solvents formed between choline chloride and carboxylic acids: versatile alternatives to ionic liquids," *J. Am. Chem. Soc.*, vol. 126, pp. 9142–9147, 2004.

[33] K. Shahbaz, F. Mjalli, M. Hashim, and I. AlNashef, "Using deep eutectic solvents based on methyl triphenyl phosphonium bromide for the removal of glycerol from palm-oil-based biodiesel," *Energy & Fuels*, no. 25, pp. 2671–2678, 2011.

[34] K. Shahbaz, S. Baroutian, F. Mjalli, M. Hashim, and I. AlNashef, "Densities of ammonium and phosphonium based deep eutectic solvents: prediction using artificial intelligence and group contribution techniques," *Thermochim. Acta*, vol. 527, pp. 59–66, 2012.

[35] Y. Hwang *et al.*, "Stability and thermal conductivity characteristics of nanofluids," *Thermochim. Acta2*, vol. 455, pp. 70–74, 2007.

[36] B. Merckx, P. Duoignon, J. Garnier, and D. Marchand, "Simplified transient hot-wire method for effective thermal conductivity measurement in geo materials: Microstructure and saturation effect," *Adv. Civ. Eng.*, vol. 2012, 2012.

[37] P. Robinson, "Practical specific heat determination by dual furnace DSC," *Perkin Elmer Application Note*. 2013.

[38] A. Nasiri, M. Shariaty-Niasar, A. Rashidi, A. Amrollahi, and R. Khodafarin, "Effect of dispersion method on thermal conductivity and stability of nanofluid," *Exp. Therm. Fluid Sci.*, vol. 35, pp. 717–723, 2011.

[39] M. Farbod, A. Ahangarpour, and S. Etemad, "Stability and thermal conductivity of water-based carbon nanotube nanofluids," *Particuology*, vol. 22, pp. 59–65, 2015.

[40] R. Fareghi-Alamdari, F. Zamani, and M. Shekarriz, "Synthesis and thermal characterization of new ammonium–imidazolium dual dicyanamide-based ionic liquids," *J. Mol. Liq.*, vol. 211, pp. 831–838, 2015.

[41] O. Yaroshchuk, S. Tomylko, O. Kovalchuk, and N. Lebovka, "Liquid crystal suspensions of carbon nanotubes assisted by organically modified Laponite nanoplatelets," *Carbon N. Y.*, vol. 68, pp. 389–398, 2014.

[42] N. Lebovka, L. Bulavin, V. Kovalchuk, I. Melnyk, and K. Repnin, "Two-step percolation in aggregating systems," *Condens. Matter Phys.*, vol. 20, 2017.

[43] C. Shih, S. Lin, M. Strano, and D. Blankschtein, "Understanding the stabilization of liquid-phase-exfoliated graphene in polar solvents: Molecular dynamics simulations and kinetic theory of colloid aggregation," *J. Am. Chem. Soc.*, vol. 114, pp. 6148–6156, 2010.

[44] W. . Wakeham, A. Nagashima, and J. . Sengers, "Measurement of the transport properties of fluids," *Exp. Thermodyn.*, vol. 3, 1991.

[45] J. Liu, F. Wang, L. Zhang, X. Fang, and Z. Zhang, "Thermodynamic properties and

thermal stability of ionic liquid-based nanofluids containing graphene as advanced heat transfer fluids for medium-to-high-temperature applications," *Renew. Energy*, vol. 63, pp. 519–523, 2014.

[46] Y. Fang *et al.*, "Synthesis and thermo-physical properties of deep eutectic solvent-based graphene nanofluids," *Nanotechnology*, vol. 7, 2016.

[47] M. Valkenburg, R. Vaughn, M. Williams, and J. Wilkes, "Thermochemistry of ionic liquid heat-transfer fluids," *Thermochim. Acta*, vol. 425, pp. 181–188, 2005.

[48] M. Hayyan, T. Aissaoui, M. Hashim, M. AlSaadi, and A. Hayyan, "Triethylene glycol based deep eutectic solvents and their physical properties," *J. Taiwan Inst. Chem. Eng.*, vol. 50, pp. 23–30, 2015.

[49] C. Nie, W. Marlow, and Y. Hassan, "Discussion of proposed mechanisms of thermal conductivity enhancement in nanofluids," *Int. J. Heat Mass Transf.*, vol. 51, pp. 1342–1348, 2008.

[50] V. Bianco, O. Manca, S. Nardini, and K. Vafai, *Heat transfer enhancement with nanofluids*. Boca Raton: CRC Press, 2015.

[51] A. Einstein, "A new determination of the molecular dimensions," *Ann. Phys. (N. Y).*, vol. 19, pp. 289–306, 1906.

[52] J. Eastman, S. Choi, S. Li, W. Yu, and L. Thompson, "Anomalously increased effective thermal conductivities of ethylene glycol-based nanofluids containing copper nanoparticles," *Appl. Phys. Lett.*, vol. 78, pp. 718–720, 2001.

[53] W. Yu, H. Xie, L. Chen, and Y. Li, "Investigation of thermal conductivity and viscosity of ethylene glycol based ZnO nanofluid," *Thermochim. Acta*, vol. 491, pp. 92–96, Jul. 2009.

[54] V. Kumaresan and R. Velraj, "Experimental investigation of the thermo-physical properties of water-ethylene glycol mixtures based CNT nanofluids," *Thermochim.*

*Acta*, vol. 545, pp. 180–186, 2012.

[55] B. Wang, L. Zhou, and X. Peng, "Surface and size effects on the specific heat capacity of nanoparticles," *Int. J. Thermophys.*, vol. 27, pp. 139–151, 2006.

[56] S. Angayarkanni, V. Sunny, and J. Philip, "Effect of nanoparticle size, morphology and concentration on specific heat capacity and thermal conductivity of nanofluids," *J. Nanofluids*, vol. 4, pp. 302–309, 2015.

[57] J. Naser, F. Mjalli, and Z. Gano, "Molar heat capacity of selected type III deep eutectic solvents," *J. Chem. Eng. Data*, vol. 61, pp. 1608–1615, 2016.

[58] J. Crosthwaire, M. Muldoon, J. Dixon, J. Anderson, and J. Brennecke, "Phase transition and decomposition temperatures, heat capacities and viscosities of pyridinium ionic liquids," *J. Chem. Thermodyn.*, vol. 37, pp. 559–568, 2005.

[59] G. Garcia, S. Aparicio, R. Ullah, and M. Atilhan, "Deep eutectic solvents: physicochemical properties and gas separation applications," *Energy & Fuels*, vol. 29, pp. 2616–2644, 2015.

[60] A. Yadav, S. Trivedi, R. Rai, and S. Pandey, "Densities and dynamic viscosities of (choline chloride+glycerol) deep eutectic solvent and its aqueous mixtures in the temperature range (283.15-363.15)K," *Fluid Phase Equilib.*, vol. 367, pp. 135–142, 2014.

[61] S. K. Das, N. Putra, P. Thiesen, and W. Roetzel, "Temperature dependence of thermal conductivity enhancement for nanofluids," *J. Heat Transfer*, vol. 125, p. 567, Aug. 2003.

[62] W. Rashmi, M. Khalid, S. Ong, and R. Saidur, "Preparation, thermo-physical properties and heat transfer enhancement of nanofluids," *Mater. Res. Express*, vol. 1, 2014.